C. R. Geoscience 349 (2017) 32–41

Contents lists available at ScienceDirect

Comptes Rendus Geoscience

www.sciencedirect.com

Stratigraphy, Sedimentology

A new biostratigraphic correlation for Late Cretaceous–Paleocene strata of the Gulf of Guinea: Evidence from dinoflagellate cysts

Raquel Sánchez-Pellicer [a,b,*], Edwige Masure [a], Loïc Villier [a]

[a] Centre de recherche sur la paléobiodiversité et les paléoenvironnements, CR2P UMR7207–CNRS, MNHN, UPMC, case 104, université Pierre-et-Marie-Curie, 75252 Paris cedex 05, France
[b] Dpto. Ciencias de la Tierra (Área Paleontología), Universidad de Zaragoza, C/Pedro Cerbuna 12, 50009 Zaragoza, Spain

ARTICLE INFO

Article history:
Received 28 October 2016
Accepted after revision 22 November 2016
Available online 15 February 2017

Handled by Sylvie Bourquin

Keywords:
Upper Cretaceous/Palaeocene
Côte d'Ivoire–Ghana
ODP Hole 959D
Biostratigraphy
Dinoflagellate cysts

ABSTRACT

A new biostratigraphic correlation for Late Cretaceous and Palaeocene strata of the Côte d'Ivoire–Ghana continental margin has been developed from the identification of significant dinoflagellate cyst events in ODP Hole 959D. The Late Cretaceous stage boundaries are mostly consistent with previous studies. However, the Maastrichtian/Danian boundary is placed much lower than previously recognized on the basis of the first occurrences of *Carpatella cornuta* and *Damassadinium californicum*. The base of the Selandian is recognized from the last occurrence of *Cerodinium diebelii* and the first occurrence of *Adnatosphaeridium multispinosum*. The base of the Thanetian is recognized from the first occurrence of *Areoligera gippingensis*. The rarity of the age-marker taxa is the main reason for different age determinations among studies of the same section.

1. Introduction

One of the most prominent events during the Cretaceous was the opening of the South Atlantic Ocean. Recent studies have focused on the palaeoceanographic and palaeoclimatic consequences of the establishment of a connection between the Central and South Atlantic (e.g., Friedrich and Erbacher, 2006). However, the precise timing of the evolution of the South Atlantic Ocean is still debated (e.g., Murphy and Thomas, 2013; Uenzelmann-Neben et al., 2016). Improving chronological constraints on the sedimentary record in marginal basins bordering the South Atlantic is essential to resolving this debate, as well as deciphering the complex palaeoceanographic and palaeoclimatic evolution of the region.

The Ocean Drilling Program (ODP) Leg 159 drilled the Côte d'Ivoire–Ghana continental margin with the goal of further understanding the early evolution of the South Atlantic (Mascle et al., 1996). Moullade et al. (1998) proposed an integrated biostratigraphic scheme for the Mesozoic combining results from various paleontological studies. As the paleomagnetic signal of the studied interval is too homogeneous to allow a precise time calibration (Allerton, 1998), biostratigraphy remains the best tool for solving the chronostratigraphic evolution of this region (Moullade et al., 1998).

In the present study, we re-analysed a subset of samples previously examined by Masure et al. (1998); the data from that work and from Oboh-Ikuenobe et al. (1998) constituted the dinoflagellate cyst data-source used by

* Corresponding author. Centre de recherche sur la paléobiodiversité et les paléoenvironnements, CR2P UMR7207–CNRS, MNHN, UPMC, case 104, université Pierre-et-Marie-Curie, 75252 Paris cedex 05, France.
E-mail address: raquel.sanchez_pellicer@courriel.upmc.fr (R. Sánchez-Pellicer).

http://dx.doi.org/10.1016/j.crte.2016.11.001

Moullade et al. (1998) in their biostratigraphic synthesis. Based on the new analyses, but considering all available data, a new biostratigraphic interpretation is herein proposed for the Late Cretaceous and the Paleocene. The new observations also test how differences in sampling strategy, sampling resolution, and frequency of age-marker taxa may alter age assignments.

2. Geographical and geological settings

The present study involves an examination of 23 samples from the interval from 1045.37 to 828.7 mbsf (metres below sea floor, Cores 67R to 44R) of ODP Hole 959D. The ODP Hole 959D is located at a water depth of 2090.7 m on a small plateau that extends just north of the top of the Côte d'Ivoire–Ghana Marginal Ridge (CIGMR, Fig. 1) on the southern flank of the Deep Ivorian Basin (DIB) (3° 37.656′N, 2° 44.149′W, Shipboard Scientific Party, 1996). During the Upper Cretaceous and the Paleocene, the studied area was ca. 7°S (Besse and Courtillot, 2002; van Hinsbergen et al., 2015). Both CIGMR and DIB were generated as a consequence of the Early Cretaceous rifting of the northern South Atlantic. The Côte d'Ivoire–Ghana transform margin represents a continuation of the Romanche Fracture Zone, which is the southern boundary of the area of final break-up between South America and Africa (Basile et al., 1998).

The lowest sample studied corresponds to the uppermost part of the lithologic subunit IVa, and the remaining 22 samples are from lithologic Unit III (Shipboard Scientific Party, 1996). The top of lithologic subunit IVa consists of beds of sandy dolostone, sandy limestone, and calcareous sandstone. The poorly sorted sandy limestone (67R-2) contains abundant foraminifers, nannofossils and scattered bivalve shell fragments in quartz sand. Lithological Unit III is composed of non-calcareous, black, massive claystone, which alternates with massive to faintly laminated lighter-grey claystone. Darker colours are associated with high content of organic matter and pyrite. In the lowermost part of lithologic Unit III (66R-CC to 66R-7, 1043.3 to 1033.7 mbsf), phosphatic hardgrounds and nodules float in a nannofossil–clayey matrix; these levels were avoided during sampling. From 1033.7 to 995.4 mbsf (Cores 65R to 61R), some slightly coarser-grained beds contain shell fragments, and plant debris occur in some laminated layers. In the uppermost part of the studied series (Core 44R, above 831 mbsf), lighter greenish-grey claystone alternates with black claystones. Bioturbated levels are present throughout the entire interval, but are more common above 990 mbsf (Shipboard Scientific Party, 1996).

3. Material and methods

All samples were processed following standard palynological preparation techniques, based on routine series of HCl–HF (70%)–HCl attacks followed by light oxidation with HNO_3 50% (Masure et al., 1998). The sampled volume was 20 ml for all samples. The organic residue was filtered through a 20-μm nylon mesh to eliminate amorphous organic matter. At least two slides were mounted in glycerine jelly from the residue of each sample. All the slides examined were previously analysed in Masure et al. (1998). As glycerine jelly dehydrates with time, some slides had to be restored before analysis. Because cover slips become brittle with age, restoration was not possible for 33 of the samples used in the original study.

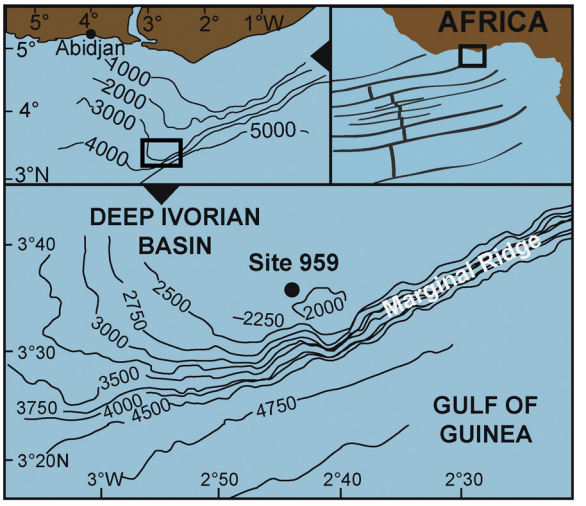

Fig. 1. Map showing the location of ODP Hole 959D in the Côte d'Ivoire–Ghana Transform Margin area. The main physiographical features in the region are indicated.
Modified from Mascle et al., 1998.

The complete list of analysed samples is shown in Table 1. All counts and scans were performed under a transmitted-light microscope (Leica DM750), the slides scanned along non-overlapping traverses using a 63x objective lens. Taxonomic identification of dinoflagellate cysts was performed using a 100x objective lens. Wherever possible, a minimum of 250 dinoflagellate cysts was counted for each level, relative abundances of taxa were calculated,

Table 1
List of samples analysed for dinoflagellate cyst assemblage composition from ODP Hole 959D.

Core	Section	cm	Depth (mbsf)
44R	6	060–062	828.7
45R	1	034–039	831.94
46R	2	018–023	842.48
47R	1	035–037	851.25
48R	3	065–068	864.25
49R	4	133–137	876.03
50R	5	098–101	886.88
51R	4	008–011	893.78
52R	3	010–013	901.91
53R	6	018–020	914.97
54R	2	097–099	920.57
55R	3	083–085	930.39
56R	4	060–062	942.5
57R	4	114–117	952.74
58R	3	093–096	960.3
59R	5	039–044	972.89
60R	1	056–059	976.66
60R	4	058–061	981.18
62R	1	076–080	996.16
63R	5	091–093	1011.91
64R	1	092–095	1015.62
66R	3	040–043	1037.1
67R	2	057–061	1045.37

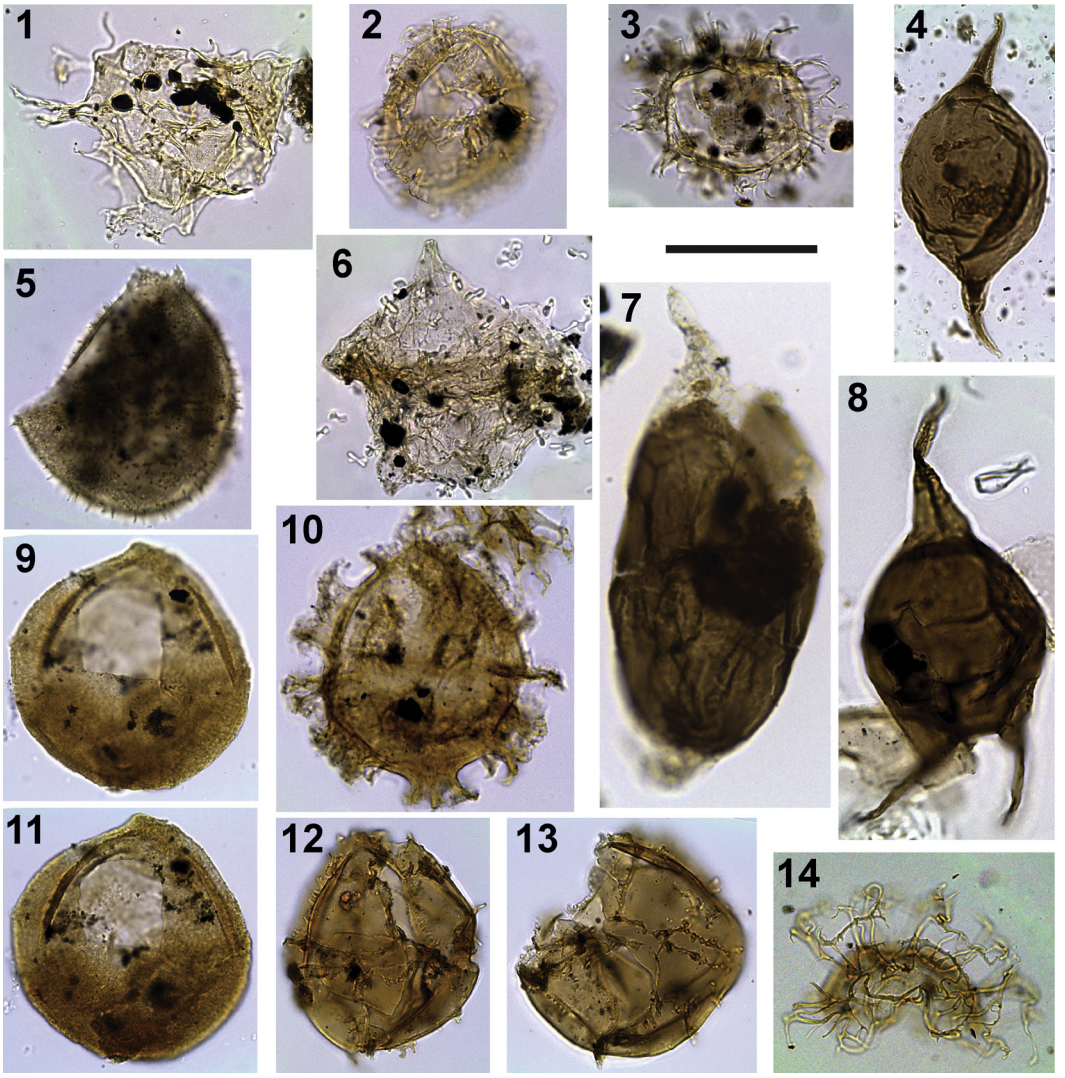

Plate 1. Photomicrographs of biostratigraphic marker taxa identified in ODP Hole 959D. All images are at the same scale; scale bar = 50 m. **1**: *Xenascus gochtii*, sample 67R02 (57–61 cm); 1045.4 mbsf, slide 1. External dorsal view. **2**: *Unipontidinium grande*, sample 64R01 (92–95 cm); 1015.62 mbsf, slide 5. Dorsal view. **3**: *Areoligera* sp., sample 62R01 (76–80 cm); 996.16 mbsf, slide 2. Apical view. **4**: *Palaeocystodinium lidiae*, sample 56R04 (60–62 cm); 942.5 mbsf, slide 3. External dorsal view. **5**: *Trichodinium castanea*, sample 58R03 (93–96 cm); 960.30 mbsf, slide 1, EF: 43P. External right lateral view. **6**: *Phelodinium magnificum*, sample 60R04 (58–61 cm); 981.18 mbsf, slide 2, EF: 40 J. Middle focus. **7**: *Andalusiella ivoirensis*. Sample 57R04 (114–117 cm); 952.74 mbsf, slide 2, EF: 28W2. External left lateral view. **8**: *Cerodinium diebelii*, sample 47R01 (35–37 cm); 851.25 mbsf, slide 1, EF: 46F3. External dorsal view. **9**, **11**: *Carpatella cornuta*, sample 52R03 (10–13 cm); 901.91 mbsf, slide 1. **9**: External dorsal view. **11**: Same specimen internal ventral view. **10**: *Damassadinium californicum*, sample 51R04 (08–11 cm); 893.78 mbsf, slide 1. Middle focus. **12**, **13**: *Impagidinium celineae*. Sample 48R03 (65–68 cm); 864.25, slide 1. **12**: 33W4, external left dorso-lateral view. Note that the operculum (Type P, 3′) is within the body cyst. **13**: EF: EF: 38P4. External right lateral view. **14**: *Adnatosphaeridium multispinosum* operculum. Sample 44R06 (60–62 cm); 828.7 mbsf, slide 2, EF: 34R2. Middle focus.

and all available slides were then scanned for additional dinoflagellate cyst taxa. The taxonomy is based on Fensome et al. (2008). Transmitted-light photomicrographs (Plate 1) were taken with a Leica ICC50 digital camera using Leica Application Suite software. All slides containing illustrated specimens are stored in the micropalaeontological collection of the "Muséum national d'histoire naturelle" (MNHN), Paris, France. England Finder (EF) coordinates of figured specimens are given in the figure captions.

4. Results

4.1. Biostratigraphy according to new dinoflagellate cyst data

From the study of the 23 samples, 125 dinoflagellate cyst taxa were identified. Fig. 3 illustrates the stratigraphic distribution of biostratigraphic markers and the most abundant dinoflagellate cyst taxa.

The biostratigraphic interpretations presented are based on new observations of First Occurrence (FO) and

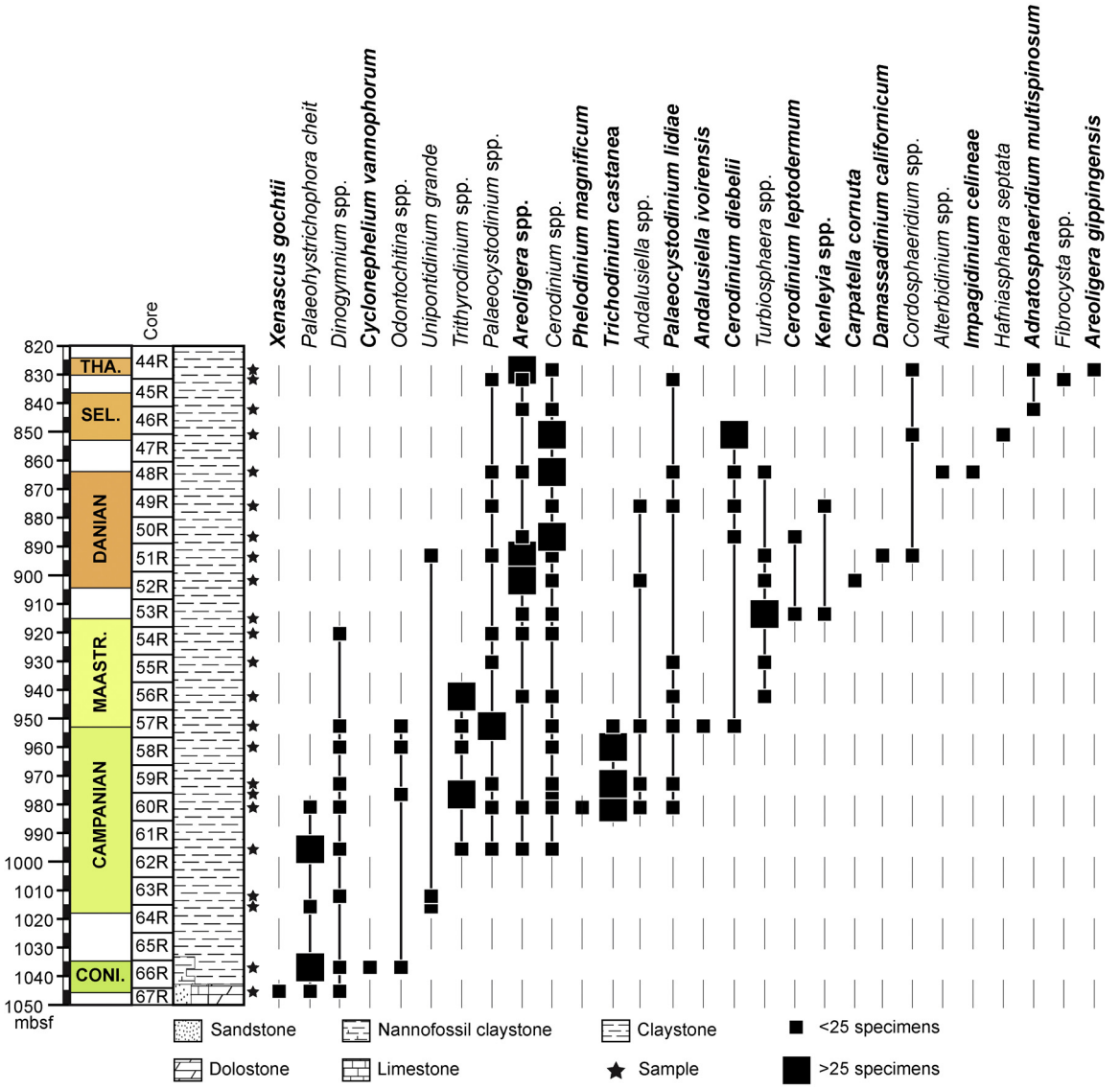

Fig. 2. Stratigraphical distribution of selected dinoflagellate cyst taxa in ODP Hole 959D. Biostratigraphy based on dinoflagellate cyst events identified in the present study. CONI: Coniacian; MAASTR: Maastrichtian; SEL: Selandian; THA: Thanetian.

Last Occurrence (LO) data of the dinoflagellate cyst identified. Age determinations in this study are based on comparison with dinoflagellate cyst assemblages described from various Turonian to Thanetian sections around the world and on the various paleontological contributions dealing with Cretaceous sediments included in Mascle et al. (1998). The following paragraphs provide an overview of the criteria for recognizing each stage.

Coniacian: the lowest occurrence of dinoflagellate cysts in the sample subset is in the uppermost sample of the lithologic Subunit IVa at 1045.37 mbsf (Fig. 2). In this sample, dinoflagellate cysts are scarce and long-ranging taxa dominate the assemblage. The only occurrence of *Cyclonephelium vannophorum* is observed at 1037.1 mbsf (Fig. 2). Since, the LO of *C. vannophorum* occurs in Coniacian strata (Williams and Bujak, 1985, p. 900, fig. 19), the interval from 1045.37 to 1037.1 mbsf is here considered as Coniacian or older in age (Fig. 2).

Santonian: no dinoflagellate cyst markers of the Santonian stage were identified during the present study.

Campanian: the base of the Campanian is suggested at 1011.91 mbsf on the basis of the FO of *Unipontidinium grande* (Fig. 2; Plate 1, Fig. 2) (Guédé et al., 2014). The FO of *Areoligera* at 996.16 mbsf confirms this age (Fig. 2; Plate 1, Fig. 3). On global charts, the FO of the *Areoligera* is considered to appear during the Campanian (Powell, 1992), and is known from the Campanian type sections (Masure, 1985), as well as from the Campanian of Gabon (Boltenhagen, 1977). The dinoflagellate cyst assemblage at 981.18 mbsf is also characteristic of the Campanian, with the presence of *Andalusiella*, *Trichodinium castanea* subsp. *bifurcatum* and *Palaeocystodinium lidiae* (Plate 1, Fig. 4); it

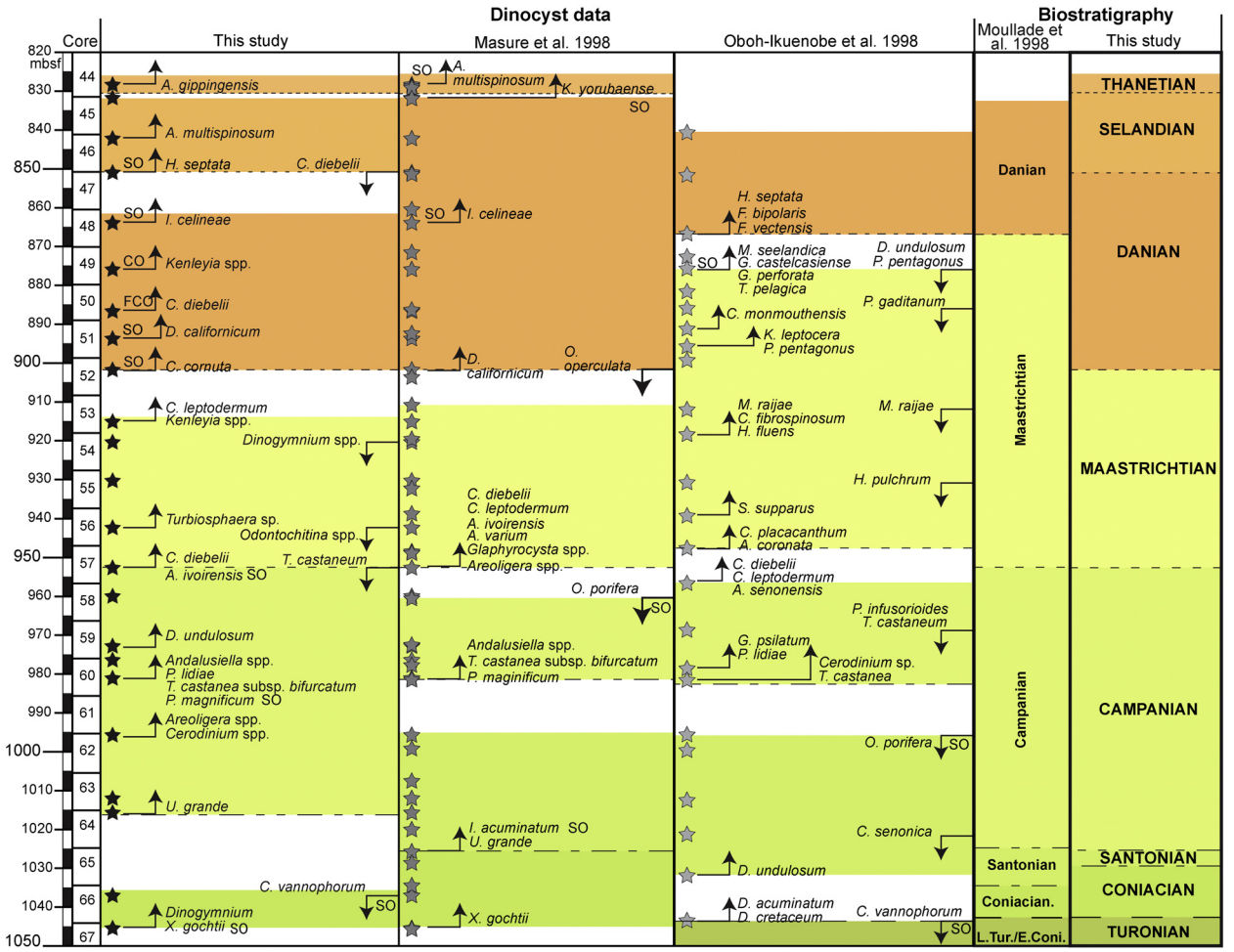

Fig. 3. Main dinoflagellate cyst events in ODP Hole 959D samples. SO: Single occurrence; CO: Common Occurrence; FCO: First Common Occurrence; up-arrows: First occurrence (FO); down-arrows: Last Occurrence (LO). Stars present in each column indicate sample positions. L. TURO./E. CONI.: Late Turonian/Early Coniacian.

also contains the only occurrence of *Phelodinium magnificum* (Fig. 2; Plate 1, Fig. 6). *Andalusiella* is known to appear during the Campanian (Williams et al., 1993); it is also known from the Campanian of Gabon (as the "*Svalbardella* group" in Boltenhagen, 1977) and Egypt (Schrank, 1987) where *T. castanea* subsp. *bifurcatum* is also present. The first appearance datum (FAD) of *P. magnificum* is Campanian in the globally based range charts of Williams and Bujak (1985, p. 901, fig. 19).

Maastrichtian: the first Maastrichtian marker, *Andalusiella ivoirensis* (Plate 1, Fig. 7), is observed at 952.74 mbsf. This taxon was first described from the Maastrichtian of the Côte d'Ivoire (Masure et al., 1996). The FO of *Cerodinium diebelii* (Plate 1, Fig. 8), and the LO of the *T. castanea* subspp. (Plate 1, Fig. 5), were also identified at 952.74 mbsf (Fig. 3). The range charts of Williams and Bujak (1985) indicate a Campanian age for FO of *Cerodinium diebelii* (p. 901, fig. 19, as *Ceratiopsis diebelii*). However, the precise age of the FO of *Cerodinium diebelii* varies slightly depending on latitude (Williams et al., 2004 and references herein). The range charts of Williams and Bujak (1985) indicate a late Campanian age for the LO of *T. castanea.* The co-occurrence of Campanian and Maastrichtian marker dinoflagellate cysts at this level suggests mixing in a condensed horizon or a hiatus between the Campanian and the Maastrichtian.

Danian: the first occurrence of Danian dinoflagellate cyst markers occurs at 901.91 mbsf, with the only occurrence of *Carpatella cornuta* (Fig. 2, Plate 1, Fig. 9–11). At 893.78 mbsf, we observed the only occurrence of *Damassadinium californicum* (Plate 1, Fig. 10). The FO of *C. cornuta* is considered a worldwide marker of the base of the Paleocene. This taxon has its FO at the base of the Danian in both the Northern Hemisphere (Brinkhuis and Leereveld, 1988; Brinkhuis and Zachariasse, 1988; Brinkhuis et al., 1998; Habib et al., 1996; Hansen, 1977, 1979a; Hultberg, 1986; Vellekoop et al., 2015; Williams et al., 1993) and the Southern Hemisphere (Willumsen, 2006, 2004, 2000). *D. californicum* is also used as a marker for the base of the Danian worldwide (Haq et al., 1987; Williams and Bujak, 1985; Williams et al., 2004). It occurs in the basal Danian in Europe (Hansen,1977, 1979a, b), Morocco

(Slimani et al., 2010), Tunisia (Brinkhuis and Zachariasse, 1988) and Alabama (Habib et al., 1992). *Impagidinium celineae* (Plate 1, Figs. 12–13), which appears at 864.25 mbsf (Fig. 2), was described from the Danian of Nigeria (Jan du Chêne, 1988; Jan du Chêne and Adediran, 1985) and Morocco (Slimani et al., 2010).

Selandian: the LO of *Cerodinium diebelii* was observed at 851.25 mbsf. This event is considered to occur at the base of the Selandian at low latitudes (Williams et al., 2004). The FO of *Adnatosphaeridium multispinosum* was observed at 842.48 mbsf (Fig. 2; Plate 1, Fig. 14). On global charts, *A. multispinosum* is considered to be restricted to the Eocene (Powell, 1992; Williams and Bujak, 1985). However, *A. multispinosum* has been identified in the late Paleocene of Nigeria (Jan du Chêne and Adediran, 1985) and of Tunisia (Kocsis et al., 2014), and its FO is considered by some authors as indicative of a Selandian age (Ogg et al., 2016).

Thanetian: the FO of *Areoligera gippingensis* at 828.7 mbsf points to a Thanetian age (Jolley, 1992; Williams et al., 2004).

4.2. New biostratigraphy

A new multidisciplinary biostratigraphy and an age-depth plot are proposed (Fig. 4). They combine the dinoflagellate cyst events recorded in this study with the biostratigraphic data published by Moullade et al. (1998 and references herein); the age associated with the biostratigraphic events is revised considering Ogg et al. (2016).

Cretaceous: the recognition of the nannofossil zone CC13 between 1050 and 1042.9 mbsf (Watkins et al., 1998) indicates a late Turonian age. *Xenascus gochtii* is observed at 1045.37 mbsf (Fig. 2; Plate 1, Fig. 1). This taxon is known to first occur during the Coniacian to the Campanian (Corradini, 1973)–more precisely Coniacian–Santonian times according to Kirsch (1991). The occurrence of *X. gochtii* within the nannofossil zone CC13 constitutes the first observation of this taxon within Turonian strata (Figs. 3 and 4). The recognition of the nannofossil zones CC14 and CC15 between 1042.8 and 1029.3 mbsf indicates a Coniacian age for this interval. The age-depth plot suggests a condensed interval for the lower Coniacian and an increase in the sedimentation rate for the upper Coniacian (Fig. 4). The identification of the nannofossil zone CC16 (Watkins et al., 1998) at 1028.5 mbsf indicates an uppermost Coniacian to Santonian age. The low slope of the age-depth plot at these levels suggests a condensed interval (Fig. 4). The first Campanian marker appears at 1025.87 mbsf (Figs. 3 and 4) on the basis of the FO of *U. grande* (Masure et al., 1998). The co-occurrence of Campanian and Maastrichtian dinoflagellate cyst events at 952.74 mbsf observed in the present study and recorded in

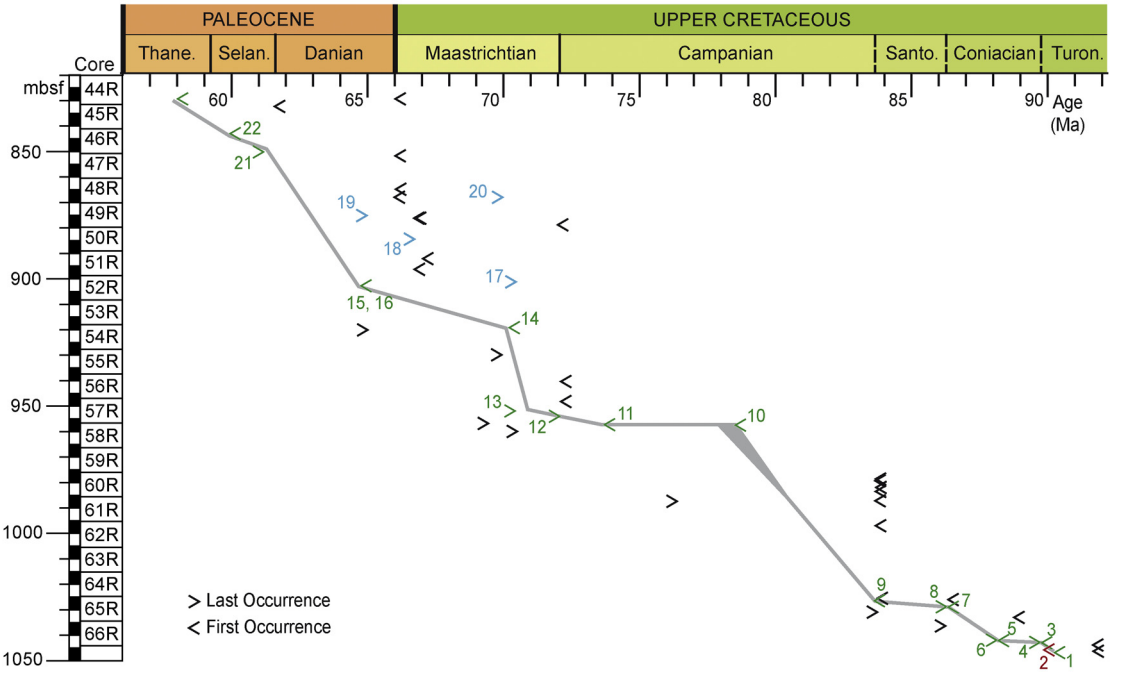

Fig. 4. Biostratigraphic age-depth plot of the ODP Hole 959D. Depth is indicated along the *y*-axis. Geologic eras are indicated along the *x*-axis. Biostratigraphical data used for the curve construction **1**: Base of the nannofossil zone CC13. **3**: Top of the nannofossil zone CC13. **4**: Base of the nannofossil zone CC14. **5**: Top of the nannofossil zone CC14. **6**: Base of the nannofossil zone CC15. **7**: Top of the nannofossil zone CC15. **8**: Base of the nannofossil zone CC16. **9**: *Unipontidinium grande* FO. **10**: *Cerodinium diebelii* FO the symbol horizontal elongation indicates the diachronism of this event between northern and southern hemisphere mid-latitudes (Williams et al., 2004). **11**. *Cerodinium leptodermum* FO. **12**: *Alterbidinium varium* FO. **13**: *Trichodinium castanea* LO. **14**: *Cordosphaeridium fibrospinosum* FO. **15**: *Carpatella cornuta* FO. **16**: *Damassadinium californicum* FO. **21**: *Cerodinium diebelii* LO at equatorial low latitudes (Williams et al., 2004). **22**: *Adanatosphaeridium multispinosum* FO. Other data. **2**: *Xenascus gochtii* FO. Evidence of reworking within the identified events **17**. *Odontochitina operculata* LO. **18**: *Phelodinium gaditanum* LO. **19**: *Dinogymnium undulosum* LO. **20**: *Caudammina gigantea* LO (agglutinated foraminifera). Turon.–Turonian, Santo.–Santonian, Selan.–Selandian, Thane.–Thanetian.

Table 2
Comparison of sampling density (mean distance between consecutive samples), position of stage boundaries (measured in metres below sea floor), "gaps" (gaps with no objective dating) and "errors" (distance between stage bases in the new biostratigraphic scheme and those stablished from the dinoflagellate cyst biostratigraphy in Masure et al. (1998), in the present study, and in Oboh-Ikuenobe et al. (1998)).

	Masure et al. (1998)			This study			Oboh-Ikuenobe et al. (1998)		
Number of studied samples	49			23			26		
Studied interval (mbsf)	1045.37–828.7			1045.37–828.7			1053.16–841.37		
Mean distance between samples (m)	4.52			9.85			8.47		
	Interval (mbsf)	Gap (m)	Error (m)	Interval (mbsf)	Gap (m)	Error (m)	Interval (mbsf)	Gap (m)	Error (m)
Recognized stages									
Thanetian	828.93–828.7	2.78	−0.23	828.7	3.24	0		8.72	
(828.7)		7.88 0			13			9.41	
Selandian		14.98		851.25–842.48	13.06	0		14.07	
(851.25–828.7)		2.81			0			11.7	
Danian	901.91–831.71		0	901.91–864.25	25.19	0	866.97–841.37		34.94
(901.91–851.25)									
Maastrichtian	960.03–910.97		−7.29	952.74–914.97		0	947.41–875.69		5.33
(952.74–901.91)									
Campanian	981.18–960.03		44.69	1011.91–952.74		13.96	981.54–956.82		44.33
(1025.87–952.74)									
Santonian	1025.87–996.16		2.63				1031.7–995.61		−3.20
(1028.5–1025.87)									
Coniacian	1045.37–1028.68		−2.81	1045.37–1037.1		−2.81	1053.16–1043.4		−10.26
(1042.9–1028.5)									
Turonian									
(1050–1042.9)									
Cumulative		28.45			54.49			43.90	

Masure et al. (1998) suggests a condensed horizon or hiatus. The age-depth plot confirms this idea (Fig. 4). Above this sample dinoflagellate cysts and agglutinated benthic foraminifers confirm a Maastrichtian age.

Paleocene: the occurrence of *C. cornuta*, this study, and *D. californicum* (Masure et al., 1998) at 901.91mbsf suggests a Danian age for this sample. Moullade et al. (1998) placed the Maastrichtian/Danian boundary at 875.69 mbsf (Fig. 3) on the basis of the LOs of *Dinogymnium undulosum* and *Pierceites pentagonus*, as well as an acme in the abundance of *Manumiella seelandica* (10%), which has its single occurrence at this level (Oboh-Ikuenobe et al., 1998). The acme of *M. seelandica* is used as a worldwide marker for the Maastrichtian–Danian boundary (Hultberg, 1986; Slimani et al., 2010; Soncini, 1990), but because it only occurs at this level, there is no way of knowing whether this occurrence represents its acme. The presence of two Paleocene dinoflagellate cyst markers below 875.69 mbsf suggests that the Maastrichtian dinoflagellate cysts used as markers (*D. undulosum* and *P. pentagonus*) may be reworked. The reworking that may have occurred in these levels is supported by the presence of pebbly mudstone beds and the highly mature nature of the contained organic matter (Wagner and Pletsch, 1999). The age-depth plot also suggests that some of the identified biostratigraphic events may be associated with reworking (Fig. 4). The base of the Selandian is placed at 851.25 mbsf based on the LO of *Cerodinium diebelii*. The base of the Thanetian is placed at 828.7 mbsf, based on the presence of *A. gippingensis*.

5. Discussion

Biostratigraphy is the key to establishing chronostratigraphic units and correlations. However, the appearance, temporal range and disappearance of taxa are not exclusively time-controlled. A number of palaeoecological, taphonomic, diagenetic and stratigraphic factors influence the geological record of the evolutionary dynamics of fossil taxa (e.g., Gradstein, 1985; Holland, 2000). The comparison of our results with those obtained by Masure et al. (1998) and Oboh-Ikuenobe et al. (1998) allows us to evaluate the main biases influencing age interpretations.

5.1. Density of sampling and biostratigraphic resolution

Intuitively, the sample density is expected to impact the placement of stage boundaries and the number and range of intervals without stage assignment (Fig. 3, Table 2). The lesser stratigraphic density of our samples prevents the identification of some stages, for example the Santonian. Masure et al. (1998) suggested a Santonian age for the FO of *Isabelidinium acuminatum* at 1025.37 mbsf (Fig. 3). Oboh-Ikuenobe et al. (1998) placed the base of the Santonian at 1031.7 mbsf based on the identification of FO of *D. undulosum*. Data revision leads us to place the Santonian boundary 2.63 m below the position suggested by Masure et al. (1998) and 3.20 m above the position suggested by Oboh-Ikuenobe et al. (1998) (Table 2). In the present study, the dinoflagellate cyst assemblage at 1025.37 mbsf was not studied; *I. acuminatum* was not

observed in any of the samples and the FO of *D. undulosum* was identified at 972.89 mbsf, within the interval dated as Campanian. The non-observation of these events in lower samples implies that we cannot define the Santonian stage from our dinoflagellate cyst dataset. The implied error for the lower Santonian boundary would reach 25.19 m in the present study (Table 2). Oboh-Ikuenobe et al. (1998) placed the top of the Coniacian at 1043.24 mbsf (Fig. 3), with the only occurrence of *C. vannophorum*, interpreted as the LO of *C. vannophorum*. In our study, the presence of *C. vannophorum* at 1037.10 mbsf leads us to suggest the upper boundary of the Coniacian at 1037.1 mbsf (Table 2). From the new multidisciplinary biostratigraphy herein proposed, the upper boundary of the Coniacian is placed at 1028.5 mbsf, thus the error on the position of the upper boundary of the Coniacian is greater in Oboh-Ikuenobe et al. (1998) than in our estimation (Table 2), despite their greater sampling density.

5.2. Rarity effect and the recognition of age-markers

Our re-analysis of the sample subset from the material studied by Masure et al. (1998) reveals that almost all dinoflagellate cyst events identified by those authors were also recorded in the present study, albeit commonly at a different stratigraphic level (Fig. 3). As would be expected, the analyses of Masure et al. (1998) also identified some dinoflagellate cyst events that were not recognized in the present study. For example, the FOs of *Glaphyrocysta* spp. and *Alterbidinium varium* at 952.74 mbsf. Several dinoflagellate cyst events that we identified were not recognized by Masure et al. (1998): the FO of *P. lidiae* at 981.18 mbsf, the FO of *C. cornuta* at 901.9 mbsf and the occurrence of *A. gippingensis* at 828.7 mbsf. When comparing the two studies, differences in the identification and placement of dinoflagellate cyst events result in the non-identification of the Selandian in Masure et al. (1998).

Among the dinoflagellate cyst events used in the three ODP Hole 959D biostratigraphic studies (Fig. 3), taxa recorded through a single occurrence are very common (e.g., *C. vannophorum*, *C. cornuta*, *I. celineae*, *M. seelandica*, Fig. 3). Combined with the high frequency of dinoflagellate cyst events established from species represented by three or fewer specimens (very rare = 2–3 specimens; present = 1 specimen), this suggests that the most useful marker taxa are also the less common (Table 3).

Chance is such a non-trivial parameter in taxon recovery and identification and in the reliability of the biostratigraphic interpretations. Within the interval common to all the studies, the most notable difference between the biostratigraphy as interpreted by us and by Moullade et al. (1998) is the displacement of the Maastrichtian–Danian boundary to a much lower level, at 901.91 mbsf, in our study (Fig. 3). The low frequency of dinoflagellate cyst markers near the boundary suggests that the controversy may simply be a result of chance in the recovery and identification of stratigraphically useful taxa.

Table 3
Frequency distribution of dinoflagellate cyst biostratigraphic markers in Oboh-Ikuenobe et al. (1998) and in the present study. The data from Masure et al. (1998) are not considered for this comparison because their publication contains exclusively presence/absence data.

Frequency dinoflagellate cyst	Total 41
Present (1 cyst)	16
Very Rare (2–3 cyst)	12
Rare (4–9 cyst)	8
Common (10–24 cyst)	4
Abundant (25–49 cyst)	1
Very Abundant (55–99 cyst)	O
Dominant (> 100 cyst)	O

5.3. Influence of paleoenvironmental factors on the dinoflagellate cyst stratigraphic record

Previous studies on the sedimentological and structural evolution of the Côte d'Ivoire–Ghana transform margin from Site 959D suggest an initial marked phase of deepening from the late Coniacian to the early Campanian (ca. 1035 to 1015 mbsf) (Basile et al., 1998; Pletsch et al., 2001; Saint-Marc and N'Da, 1997; Wagner and Pletsch, 1999). The high contribution of marine, fluorescent organic matter in samples from this interval has been interpreted as representing shallow-water conditions (Oboh-Ikuenobe et al., 1998; Pletsch et al., 2001). The composition of benthic foraminifer assemblages suggests an extended oxygen minimum zone in the water column during the Coniacian and an increase in water depth during the Santonian (Holbourn and Kuhnt, 1998; Pletsch et al., 2001). The deepening rate was lower and almost constant during most of the Campanian–Maastrichtian interval. From the early Campanian on, the sea floor had subsided sufficiently to allow the initiation of deep-water circulation (Friedrich and Erbacher, 2006; Pletsch et al., 2001; Saint-Marc and N'Da, 1997). During this last interval, sediments were enriched in mixed marine/continental and oxidized organic matter, a condition consistent with deep environments (Pletsch et al., 2001; Wagner and Pletsch, 1999). From the analysis of sedimentological, mineralogical, micropalaeontological and organic geochemical data, Pletsch et al. (2001) proposed that depth remained stable for the entire Paleogene (from ca. 890 mbsf to the top of the studied interval). Paleoenvironmental control on the relative frequency of dinoflagellate cyst taxa may impact the stratigraphic interpretation. Environmental changes have been proposed to explain variations in dinoflagellate cyst distribution in sedimentary sequences. Sea-surface temperature variations have been proposed as triggers of variations in dinoflagellate cyst frequency across the Cretaceous/Paleogene boundary in different regions. For example, Brinkhuis et al. (1998) and Vellekoop et al. (2015) found that some biostratigraphic markers (such as *Palynodinium grallator*, *P. pentagonus*, *P. magnificum* and *Senegalinium bicavatum*) are influenced by SST variations. Improving our understanding of how paleoenvironmental variation controls dinoflagellate cyst distribution is fundamental to realizing the full potential of dinoflagellate cyst as biostratigraphic markers.

6. Conclusions

The new analysis of the dinoflagellate cyst from the Upper Cretaceous to Paleocene interval in ODP Hole 959D

on the Côte d'Ivoire–Ghana continental margin leads us to propose a new comprehensive biostratigraphy. The positions of the boundaries between Cretaceous stages mostly coincide with those recognized by Moullade et al. (1998). The age of biostratigraphic events is revised. The identification of new dinoflagellate cyst events has allowed us to place the Maastrichtian/Danian boundary lower than in Moullade et al. (1998) and to recognize the Danian/Selandian, at 901.91 mbsf, and Selandian/Thanetian boundaries respectively at 851.25 mbsf and 828.7 mbsf. Our results offer a new biostratigraphic correlation for the Cretaceous and Palaeocene of the Gulf of Guinea that minimizes the risk of error in the placing of stage boundaries and affirms the value of multidisciplinary approaches.

The comparison of our data with those published by Masure et al. (1998) and Oboh-Ikuenobe et al. (1998) from the same interval allows some discussion on the basis of biostratigraphy. We consider low sampling resolution and the rarity of markers to be the main factors determining the significant differences in boundaries placement.

The relative abundance distribution of dinoflagellate cysts suggests that environmental conditions may influence their stratigraphic range. However, because of the complexity of paleoenvironmental signal registered by the fossil record, further work is necessary to assess the potential of fossil dinoflagellate cysts as paleoenvironmental proxies.

Acknowledgements

R.S.P. thanks Daniel Michoux for his helps on dinoflagellate cyst systematic and taxonomy. and Jean Dejax for sharing his knowledge on restoring palynological slides. Funding for this research was provided by TOTAL. The samples were provided by the Ocean Drilling Program (ODP), an organization sponsored by the U.S. National Science Foundation (NSF) and participating countries under management of Joint Oceanographic Institutions (JOI), Inc. We would like to thank Robert Fensome and Peter Bijl for their useful and constructive comments on the manuscript.

References

Allerton, S., 1998. Paleomagnetic results from Holes 959D and 960A, Côte d'Ivoire–Ghana Transfrom Margin. In: Mascle, J., Lohmann, G.P., Moullade, M. (Eds.), Proceedings of the Ocean Drilling Program, Scientific Results. College Station, TX (Ocean Drilling Program) pp. 199–207.

Basile, C., Mascle, J., Benkhelil, J., Bouillin, J.-P., 1998. Geodynamic evolution of the Côte d'Ivoire–Ghana transform margn: an overview of Leg 159 results. In: Mascle, J., Lohmann, G.P., Moullade, M. (Eds.), Proceedings of the Ocean Drilling Program, Scientific Results. College Station, TX (Ocean Drilling Program) pp. 101–110.

Besse, J., Courtillot, V., 2002. Apparent and true polar wander and the geometry of the geomagnetic field over the last 200 Myr. J. Geophys. Res. Solid Earth 107,, http://dx.doi.org/10.1029/2000JB000050 [EPM 6–1].

Boltenhagen, E., 1977. Microplancton du Crétacé Supérieur du Gabon, Cahiers de paléontologie. Centre national de la recherche scientifique, Paris.

Brinkhuis, H., Leereveld, H., 1988. Dinoflagellate cysts from the Cretaceous/Tertiary boundary sequence of El Kef, Northwest Tunisia. Rev. Palaeobot. Palynol. 56, 5–19, http://dx.doi.org/10.1016/0034-6667(88)90071-1.

Brinkhuis, H., Zachariasse, W.J., 1988. Dinoflagellate cysts, sea level changes and planktonic foraminifers across the Cretaceous-Tertiary boundary at El Haria, northwest Tunisia. Mar. Micropaleontol. 13, 153–191, http://dx.doi.org/10.1016/0377-8398(88)90002-3.

Brinkhuis, H., Bujak, J., Smit, J., Versteegh, G.J., Visscher, H., 1998. Dinoflagellate-based sea surface temperatura reconstructions across the Cretaceous_Tertiary boundary. Paleogeogr. Paleoclimatol. Paleoecol. 141, 67–83, http://dx.doi.org/10.1016/S0031-0182(98)00004-2.

Corradini, D., 1973. Non-calcareous microplankton from the Upper Cretaceous of the northern Apennines. Boll. Della Soc. Paleontol. Ital. 11, 119–197.

Fensome, R.A., MacRae, G.L., Williams, G.L., 2008. DINOFLAJ2, Version 1. Am. Assoc. Stratigr. Palynol. Data Ser. 1 .

Friedrich, O., Erbacher, J., 2006. Benthic foraminiferal assemblages from Demerara Rise (ODP Leg 207, western tropical Atlantic): possible evidence for a progressive opening of the Equatorial Atlantic Gateway. Cretaceous Res. 27, 377–397, http://dx.doi.org/10.1016/j.cretres.2005.07.006.

Gradstein, F.M., 1985. Stratigraphy and the fossil record. In: Gradstein, F.M., Agterberg, F.P., Brower, J.C., Schwarzacher, W.S. (Eds.), Quantitative Stratigraphy. UNESCO, Paris, pp. 17–39.

Guédé, K.É., Slimani, H., Louwye, S., Asebriy, L., Toufiq, A., Ahmamou, M., Hassani, I.-E.E.A.E., Digbehi, Z.B., 2014. Organic-walled dinoflagellate cysts from the Upper Cretaceous–lower Paleocene succession in the western External Rif, Morocco: New species and new biostratigraphic results. Geobios 47, 291–304, http://dx.doi.org/10.1016/j.geobios.2014.06.006.

Habib, D., Moshkovitz, S., Kramer, C., 1992. Dinoflagellate and calcareous nannofossil response to sea-level change in Cretaceous-Tertiary boundary sections. Geology 20, 165–168, http://dx.doi.org/10.1130/0091-7613(1992)020<0165:DACNRT>2.3.CO;2.

Habib, D., Olsson, R.K., Liu, C., Moskovitz, S., 1996. High-resolution biostratigraphy of sea-level low, biotic extinction, and chaotic sedimentation at the Cretaceous-Tertiary boundary in Alabama, north of the Chicxulub Crater. In: Special Paper 307: the Cretaceous-Tertiary Event and Other Catastrophes in Earth History. Geological Society of America, 243–252.

Hansen, J.M., 1979a. Dinoflagellate zonation around the boundary. In: Birkelund, T., Bromley, R.G. (Eds.), Cretaceous-Tertiary Boundary Events Symposium: 1. On the Maastrichtian and Danian of Denmark. University of Copenhagen, Copenhagen.

Hansen, J.M., 1979b. A new dinoflagellate zone at the Maastrichtian/Danian boundary in Denmark. Dan. Geol. Unders. 131–140.

Hansen, J.M., 1977. Dinoflagellate stratigraphy and echinoid distribution in Upper Maastrichtian and Danian deposits from Denmark. Bull. Geol. Soc. Den. 26, 1–26.

Haq, B.U., Hardenbol, J., Vail, P.R., 1987. Chronology of fluctuating sea levels since the Triassic. Science 235, 1156–1167, http://dx.doi.org/10.1126/science.235.4793.1156.

Holbourn, A.E.L., Kuhnt, W., 1998. Turonian-Santonian benthic foraminifer assemblages from site 959D (Côte d'Ivoire-Ghana transform margin, equatorial Atlantic): indication of a Late Cretaceous oxygen minimum zone. In: Mascle, J., Lohmann, G.P., Moullade, M. (Eds.), Proceedings of the Ocean Drilling Program, Scientific Results. College Station, TX (Ocean Drilling Program) pp. 375–388.

Holland, S.M., 2000. The quality of the fossil record: a sequence stratigraphic perspective. Paleobiology 26, 148–168.

Hultberg, S.U., 1986. Danian dinoflagellate zonation, the C-T boundary and the stratigraphical position of the fish clay in southern Scandinavia. J. Micropalaeontol. 5, 37–47, http://dx.doi.org/10.1144/jm.5.1.37.

Jan du Chêne, R., 1988. Étude systématique des kystes de dinoflagelllés de la Formation des Madeleines (Danien du Sénégal). Cah. Micropaleontol. 2, 147–174.

Jan du Chêne, R., Adediran, S.A., 1985. Late Paleocene to Early Eocene dinoflagellates from Nigeria. Cah. Micropaleontol. 3, 5–38.

Jolley, D.W., 1992. Palynofloral association sequence stratigraphy of the Palaeocene Thanet Beds and equivalent sediments in eastern England. Rev. Palaeobot. Palynol. 74, 207–237, http://dx.doi.org/10.1016/0034-6667(92)90008-5.

Kirsch, K.H., 1991. Dinoflagellaten-Zysten aus der Oberkreide des Helvetikums und Nordultrahelveticums von Oberbayern. Müncher Geowiss. Abh. Reihe Geol. Palaeontol. 22, 1–306.

Kocsis, L., Ounis, A., Baumgartner, C., Pirkenseer, C., Harding, I.C., Adatte, T., Chaabani, F., Neili, S.M., 2014. Paleocene–Eocene palaeoenvironmental conditions of the main phosphorite deposits (Chouabine Formation) in the Gafsa Basin, Tunisia. J. Afr. Earth Sci. 100, 586–597, http://dx.doi.org/10.1016/j.jafrearsci.2014.07.024.

Mascle, J., Lohmann, G.P., Clift, P.D., Shipboard Scientific Party, 1996. Proceedings of the Ocean Drilling Program, Initial Reports. Ocean Drilling Program. College Station, TX, USA.

Mascle, J., Lohmann, G.P., Moullade, M., et al., 1998. Proceedings of the Ocean Drilling Program, Scientific Results. Ocean Drilling Program. College Station, TX, USA.

Masure, E., 1985. Les kystes de dinoflagellés de l'Autoroute A 10. Cretaceous Res. 6, 199–206, http://dx.doi.org/10.1016/0195-6671(85)90045-X.

Masure, E., Rauscher, R., Dejax, J., Schuler, M., Ferré, B., 1998. Cretaceous–Paleocene palynology from the Côte d'Ivoire-Ghana transform margin, sites 959, 960, 961, and 962. In: Mascle, J., Lohmann, G.P., Moullade, M. (Eds.), Proceedings of the Ocean Drilling Program, Scientific Results. College Station, TX, USA (Ocean Drilling Program), pp. 253–276.

Masure, E., Tea, J., Yao, R., 1996. The dinoflagellate *Andalusiella*: emendation of the genus, revision of species, *A. ivoirensis* Masure, Tea and Yao, sp. nov. Rev. Palaeobot. Palynol. 91, 171–186, http://dx.doi.org/10.1016/0034-6667(95)00061-5.

Moullade, M., Watkins, D.K., Oboh-Ikuenobe, F.E., Bellier, J.-P., Masure, E., Holbourn, A.E.L., Erbacher, J., Kuhnt, W., Pletsch, T., Kaminski, M.A., Rauscher, R., Shafik, S., Yepes, O., Dejax, J., Gregg, J.M., Shin, I.C., Schuler, M., 1998. Mesozoic biostratigraphic, paleoenvironmental, and paleobiogeographic synthesis, equatorial Atlantic. In: Mascle, J., Lohmann, G.P., Moullade, M. (Eds.), Proceedings of the Ocean Drilling Program, Scientific Results. College Station, TX, USA (Ocean Drilling Program) pp. 481–490.

Murphy, D.P., Thomas, D.J., 2013. The evolution of Late Cretaceous deep-ocean circulation in the Atlantic basins: Neodymium isotope evidence from South Atlantic drill sites for tectonic controls. Geochem. Geophys. Geosystems 14, 5323–5340, http://dx.doi.org/10.1002/2013GC004889.

Oboh-Ikuenobe, F.E., Yepes, O., Gregg, J.M., 1998. Palynostratigraphy, palynofacies, and thermal maturation of Cretaceous–Paleocene sediments from the Côte d'Ivoire-Ghana transform margin. In: Mascle, J., Lohmann, G.P., Moullade, M. (Eds.), Proceedings of the Ocean Drilling Program, Scientific Results. College Station, TX, USA (Ocean Drilling Program) pp. 277–318.

Ogg, J.G., Ogg, G., Gradstein, F.M., 2016. A concise geologic time scale, 1st ed. Elsevier.

Pletsch, T., Erbacher, J., Holbourn, A.E.L., Kuhnt, W., Moullade, M., Oboh-Ikuenobede, F.E., Söding, E., Wagner, T., 2001. Cretaceous separation of Africa and South America: the view from the West African margin (ODP Leg 159). J. South Am. Earth Sci. 14, 147–174, http://dx.doi.org/10.1016/S0895-9811(01)00020-7.

Powell, A.J., 1992. A Stratigraphic Index of Dinoflagellate Cysts. Chapman and Hall, London.

Saint-Marc, P., N'Da, V., 1997. Biostratigraphie et paléoenvironnements des dépôts crétacés au large d'Abidjan (Golfe de Guinée). Cretaceous Res. 18, 545–565.

Schrank, E., 1987. Paleozoic and Mesozoic palynomorphs from Northeast Africa (Egypt and Sudan) with special reference to Late Cretaceous pollen and dinoflagellates. Berl. Geowiss. Abh. A 75, 249–310.

Shipboard Scientific Party, 1996. Site 959. In: Mascle, J., Lohmann, G.P., Clift, P.D. (Eds.), Proceedings of the Ocean Drilling Program, Initial Reports. College Station, TX (Ocean Drilling Program) pp. 65–150.

Slimani, H., Louwye, S., Toufiq, A., 2010. Dinoflagellate cysts from the Cretaceous–Paleogene boundary at Ouled Haddou, southeastern Rif, Morocco: biostratigraphy, paleoenvironments and paleobiogeography. Palynology 34, 90–124, http://dx.doi.org/10.1080/01916121003629933.

Soncini, M.-J., 1990. Palynologie des Phosphates des Oulad Abdoun (Maroc). Biostratigraphie et Environnements de la Phosphatogenèse dans le Cadre de la Crise Crétacé–Tertiaire. (Thèse). Université Louis Pasteur, Strasbourg, France.

Uenzelmann-Neben, G., Weber, T., Grützner, J., Thomas, M., 2016. Transition from the Cretaceous ocean to Cenozoic circulation in the western South Atlantic – A twofold reconstruction. Tectonophysics, http://dx.doi.org/10.1016/j.tecto.2016.05.036.

van Hinsbergen, D.J.J., de Groot, L.V., van Schaik, S.J., Spakman, W., Bijl, P.K., Langereis, C.G., Brinkhuis, H., 2015. A paleolatitude calculator for paleoclimate studies. PLos ONE 10, 21, http://dx.doi.org/10.5281/zenodo.16166.

Vellekoop, J., Smit, J., van de Schootbrugge, B., Weijers, J.W.H., Galeotti, S., Sinninghe Damsté, J.S., Brinkhuis, H., 2015. Palynological evidence for prolonged cooling along the Tunisian continental shelf following the K–Pg boundary impact. Palaeogeogr. Palaeoclimatol. Palaeoecol. 426, 216–228, http://dx.doi.org/10.1016/j.palaeo.2015.03.021.

Wagner, T., Pletsch, T., 1999. Tectono-sedimentary controls on Cretaceous black shale deposition along the opening Equatorial Atlantic Gateway (ODP Leg 159). In: Cameron, N.R., Bate, R.H., Clure, V.S. (Eds.), The Oil and Gas Habitats of the South Atlantic, Special Publications. Geological Society, London, pp. 241–265.

Watkins, D.K., Shafik, S., Shin, I.C., 1998. Calcareous nannofossils from the Cretaceous of the Deep Ivorian Basin. In: Mascle, J., Lohmann, G.P., Moullade, M. (Eds.), Proceedings of the Ocean Drilling Program, Scientific Results. College Station, TX (Ocean Drilling Program) pp. 319–333.

Williams, G.L., Bujak, J.P., 1985. Mesozoic and Cenozoic dinoflagellates. In: Bolli, H.M., Saunders, J.B., Perch-Nielsen, K. (Eds.), Plankton Stratigraphy. Cambridge Univ. Press, Cambridge, UK, pp. 847–964.

Williams, G.L., Brinkhuis, H., Pearce, M.A., Fensome, R.A., Weegink, J.W., 2004. Southern Ocean and global dinoflagellate cyst events compared: index events for the Late Cretaceous–Neogene. In: Exon, N.F., Kennett, J.P., Malone, M.J. (Eds.), Proceedings of the Ocean Drilling Program, Scientific Results. College Station, TX (Ocean Drilling Program) pp. 1–98.

Williams, G.L., Stover, L.E., Kidson, E.J., 1993. Morphology and stratigraphic ranges of selected Mesozoic – Cenozoic dinoflagellate taxa in the Northern Hemisphere. Geol. Surv. Can. Pap. 92, 1–137.

Willumsen, P.S., 2000. Late Cretaceous to early Paleocene palynological changes in mid latitude Southern Hemisphere, New Zealand. GFF Geol. Fören. Stockh. Förh. 122, 180–181.

Willumsen, P.S., 2004. Two new species of the dinoflagelate cyst genus *Carpatella* Grogorovich 1969 from the Cretaceous/Tertiary transition in New Zealand. J. Micropalaeontol. 23, 119–125.

Willumsen, P.S., 2006. *Palynodinium minus* sp. nov., a new dinoflagellate cyst from the Cretaceous–Paleogene transition in New Zealand; its significance and palaeoecology. Cretac. Res. 27, 954–963, http://dx.doi.org/10.1016/j.cretres.2006.06.002.